Progress In Electromagnetics Research M, Vol. 8, 51–65, 2009

TRANSIENT ELECTROMAGNETIC FIELDS IN A CAVITY WITH DISPERSIVE DOUBLE NEGATIVE MEDIUM

M. S. Antyufeyeva and A. Y. Butrym

Department of Theoretical Radiophysics
Karazin Kharkiv National University
4 Svobody Sq., Kharkov 61077, Ukraine

O. A. Tretyakov

Department of Electronics
Gebze Institute of Technology
101 Cayirova, Gebze, Kocaeli 41400, Turkey

Abstract—Electromagnetic fields in a cavity filled with double negative dispersive medium and bounded by a closed perfectly conducting surface is studied in the Time Domain. The sought electromagnetic fields are found in a closed form by using decomposition over cavity modes and solving in TD the differential equations for the time varying mode amplitudes. Some features of frequency response of such an electromagnetic system are presented. Waveforms of electromagnetic fields excited by a wideband pulse are considered.

1. INTRODUCTION

Recently many researchers develop and create new materials with special electromagnetic properties not met in nature, known as metamaterials. Among such media an important place occupies so-called left-handed or double negative (DNG) media [1–7]. As an example of possible application of DNG medium in cavity devices we can mention a subwavelength resonator that comprises of double positive (DPS) and DNG slabs that compensate each other to provide zero total phase shift [3, 6, 8–10]. Such resonators exhibit interesting spectrum properties that among others create some problems for

Corresponding author: M. S. Antyufeyeva (Mariya.Antyufeyeva@gmail.com).

numerical analysis [11]. In order to treat DNG media properly one should always take into account dispersion of the refractive index.

A cavity filled with dispersive medium is an oscillating system composed of oscillating charges in medium and oscillating fields bounded by the cavity walls. Interaction of these oscillators within the cavity results in some interesting phenomena that we are going to study in this paper.

We consider a cavity homogeneously filled with dispersive DNG medium. For an oscillator it is important to have low losses at resonances. Since of interest is the frequency range with negative refractive index we choose such dispersion in medium so that the losses in this range are small. The dispersion models that can be easily presented both in FD and TD are based on rational fractions presentation in FD that corresponds to damping harmonic functions in TD. Among simplest models of this kind are constant conductivity, Drude, Debye, Lorentz, and their linear combinations. Drude model yields negative real part of the constitutive parameter in frequency band from 0 to some zero-crossing frequency, in the vicinity of which losses are rather small. This model properly describes permittivity behavior of many metals (conductors) in low frequency region (up to infrared). Meanwhile Drude model yields nonzero conductivity currents at DC that's why it is not appropriate for modeling permeability. That's why we choose Lorentz model for permeability. Such a model consisting of Drude permittivity and Lorentz permeability is frequently used in modeling DNG media [4]. In the Frequency Domain (FD) these dispersions can be expressed as follows

$$\varepsilon(\omega) = 1 + \frac{\chi_e \omega_e^2}{i\omega\left(i\omega + \gamma_e\right)}, \tag{1}$$

$$\mu(\omega) = 1 + \frac{\chi_m \omega_m^2}{\omega_m^2 - \omega^2 + i\omega\gamma_m}. \tag{2}$$

The model parameters are given in Fig. 1. They were chosen rather arbitrary within physical constraints so that to provide double negative refractive index $n'(f) < 0$ in some frequency region around 6–12 GHz with relatively low losses.

This medium can be described in TD by the following constitutive relations in the form of ordinary differential equations (ODE) relating electric $\mathcal{P}$ and magnetic $\mathcal{M}$ dipole moments per unit volume with the corresponding field quantities $\mathcal{E}$ and $\mathcal{H}$

$$\partial_t^2 \mathcal{P} + \gamma_e \partial_t \mathcal{P} = \varepsilon_0 \chi_e \omega_e^2 \mathcal{E}, \tag{3}$$

$$\partial_t^2 \mathcal{M} + \gamma_m \partial_t \mathcal{M} + \omega_m^2 \mathcal{M} = \chi_m \omega_m^2 \mathcal{H}\left(\mathbf{r}, t\right). \tag{4}$$

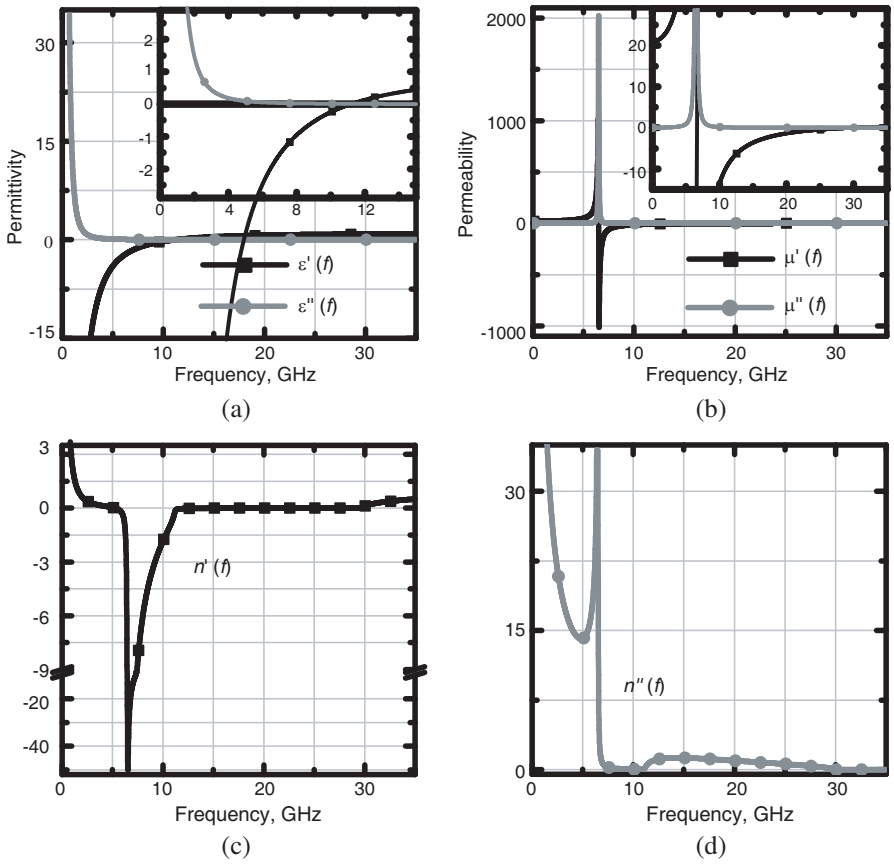

Figure 1. Frequency dependencies of permittivity, permeability and refractive index for model parameters $\chi_e = 5$, $\gamma_e/2\pi = 6 \times 10^8\,\mathrm{s}^{-1}$, $f_{e=\omega_e/2\pi} = 5\,\mathrm{GHz}$, $\chi_m = 20\gamma_m/2\pi = 4 \times 10^8\,\mathrm{s}^{-1}$, $f_{m=\omega_m/2\pi} = 6.5\,\mathrm{GHz}$.

We are going to study electromagnetic fields in a cavity with such medium and consider frequency response of this system as well as some transient effects occurring under pulse excitation in the cavity.

2. CLOSED-FORM SOLUTION TO THE PROBLEM BY MODE EXPANSION IN TIME DOMAIN METHOD

The cavity under study is bounded with a singly-connected closed PEC surface. Within the frame of Evolutionary Approach to Electromagnetics in TD [12–14] (Mode Expansion in TD) the sought

electromagnetic fields $\mathcal{E}(\mathbf{r},t)$, $\mathcal{H}(\mathbf{r},t)$, dielectric polarization $\mathcal{P}(\mathbf{r},t)$, and magnetization $\mathcal{M}(\mathbf{r},t)$ are expanded into series in terms of cavity modes:

$$\mathcal{E}(\mathbf{r},t)=\sum_{n=1}^{\infty}e_n(t)\mathbf{E}_n(\mathbf{r})-\sum_{\alpha=1}^{\infty}a_\alpha(t)\nabla\Phi_\alpha(\mathbf{r}), \tag{5}$$

$$\mathcal{H}(\mathbf{r},t)=\sum_{n=1}^{\infty}h_n(t)\mathbf{H}_n(\mathbf{r})-\sum_{\beta=1}^{\infty}b_\beta(t)\nabla\Psi_\beta(\mathbf{r}), \tag{6}$$

$$\varepsilon_0^{-1}\mathcal{P}(\mathbf{r},t)=\sum_{n=1}^{\infty}p_n(t)\mathbf{E}_n(\mathbf{r})-\sum_{\alpha=1}^{\infty}q_\alpha(t)\nabla\Phi_\alpha(\mathbf{r}), \tag{7}$$

$$\mathcal{M}(\mathbf{r},t)=\sum_{n=1}^{\infty}m_n(t)\mathbf{H}_n(\mathbf{r})-\sum_{\alpha=1}^{\infty}g_\beta(t)\nabla\Psi_\beta(\mathbf{r}). \tag{8}$$

The solenoidal cavity modes can be found as solutions to the following boundary eigenvalue problems

$$\begin{cases}\nabla\times\mathbf{H}_n(\mathbf{r})=-i\omega_n\varepsilon_0\mathbf{E}_n(\mathbf{r})\\ \nabla\times\mathbf{E}_n(\mathbf{r})=i\omega_n\mu_0\mathbf{H}_n(\mathbf{r})\\ \mathbf{n}\times\mathbf{E}_n(\mathbf{r})|_S=0 \text{ or } \mathbf{n}\cdot\mathbf{H}_n(\mathbf{r})|_S=0\end{cases} \tag{9}$$

Irrotational modes occurring in the expansions correspond to transient Coulomb and Ampère fields in the bounded cavity that are closely coupled with charges and currents. They are defined by the following eigenvalue problems

$$\left(\nabla^2+\eta_\alpha^2\right)\Phi_\alpha=0,\ \Phi_\alpha|_S=0 \text{ and } \left(\nabla^2+\nu_\alpha^2\right)\Psi_\beta=0,\ \tfrac{\partial}{\partial\mathbf{N}}\Psi_\beta\big|_S=0. \tag{10}$$

Time dependences of the fields are described by the mode amplitudes $e_n(t)$, $h_n(t)$, $p_n(t)$, $m_n(t)$, $a_\alpha(t)$, $b_\beta(t)$, $q_\alpha(t)$, $g_\beta(t)$. In the same way one can expand the initial fields as well as the impressed electric and magnetic currents $\mathcal{J}_e(\mathrm{r},t)$ and $\mathcal{J}_h(\mathrm{r},t)$

$$\mathcal{E}_0(\mathbf{r})=\sum_{n=1}^{\infty}e_n^0\mathbf{E}_n(\mathbf{r})-\sum_{\alpha=1}^{\infty}a_\alpha^0\nabla\Phi_\alpha(\mathbf{r}), \tag{11}$$

$$\mathcal{H}_0(\mathbf{r})=\sum_{n=1}^{\infty}h_n^0\mathbf{H}_n(\mathbf{r})-\sum_{\beta=1}^{\infty}b_\beta^0\nabla\Psi_\beta(\mathbf{r}), \tag{12}$$

$$\varepsilon_0^{-1}\mathcal{J}_e(\mathbf{r},t)=\sum_{n=1}^{\infty}j_n^e(t)\mathbf{E}_n(\mathbf{r})-\sum_{\alpha=1}^{\infty}j_\alpha^e(t)\nabla\Phi_\alpha(\mathbf{r}), \tag{13}$$

$$\mu_0^{-1}\mathcal{J}_h(\mathbf{r},t)=\sum_{n=1}^{\infty}j_n^h(t)\mathbf{H}_n(\mathbf{r})-\sum_{\beta=1}^{\infty}j_\beta^h(t)\nabla\Psi_\beta(\mathbf{r}), \tag{14}$$

By substituting expansions (5)–(8) and (11)–(14) into Maxwell equations and constitutive relation (3) and (4), and further applying the orthogonality conditions

$$\tfrac{\varepsilon_0}{V}\int\limits_V\mathbf{E}_n(\mathbf{r})\cdot\mathbf{E}_m^*(\mathbf{r})\,dV=\tfrac{\mu_0}{V}\int\limits_V\mathbf{H}_n(\mathbf{r})\cdot\mathbf{H}_m^*(\mathbf{r})\,dV=\delta_{nm}, \tag{15}$$

$$-\tfrac{\varepsilon_0}{V}\int\limits_V\mathbf{E}_n(\mathbf{r})\cdot\nabla\Phi_\alpha^*(\mathbf{r})dV=-\tfrac{\mu_0}{V}\int\limits_V\mathbf{H}_n(\mathbf{r})\cdot\nabla\Psi_\beta^*(\mathbf{r})dV=0, \tag{16}$$

one can obtain a system of ODEs for the mode amplitudes (known as evolutionary equations [12–14]). It can be written in a matrix form as follows:

$$\frac{d}{dt}\mathbf{X}(t)+\mathbf{Q}_{sol}\cdot\mathbf{X}(t)=\mathbf{F}_{sol}(t),\quad \mathbf{X}(t)|_{t=0}=\mathbf{X}_0, \tag{17}$$

$$\frac{d}{dt}\mathbf{Y}^e(t)+\mathbf{Q}_{irr}^e\cdot\mathbf{Y}^e(t)=\mathbf{F}_{irr}^e(t),\quad \mathbf{Y}^e(t)|_{t=0}=\mathbf{Y}_0^e, \tag{18}$$

$$\frac{d}{dt}\mathbf{Y}^h(t)+\mathbf{Q}_{irr}^h\cdot\mathbf{Y}^h(t)=\mathbf{F}_{irr}^h(t),\quad \mathbf{Y}^h(t)\Big|_{t=0}=\mathbf{Y}_0^h, \tag{19}$$

where

$$\begin{aligned}
\mathbf{X}(t)&=\mathrm{col}\left(e_n,ih_n,p_n',im_n,im_n'\right),\\
\mathbf{X}_0&=\mathrm{col}\left(e_n^0,ih_n^0,p_n'(0),im_n^0,im_n'(0)\right),\\
p_n'(t)&=\partial_t p_n(t),\ \ m_n'=\partial_t m_n,\ \ q_\alpha'=\partial_t q_\alpha,\ \ g_\beta'=\partial_t g_\beta,\\
\mathbf{F}_{sol}(t)&=\mathrm{col}\left(-j_n^e,-ij_n^h,0,0,0,0\right),\\
\mathbf{Y}^e(t)&=\mathrm{col}\left(a_\alpha,q_\alpha'\right),\quad \mathbf{Y}^h(t)=\mathrm{col}\left(b_\beta,g_\beta'\right),\\
\mathbf{Y}_0^e&=\mathrm{col}\left(a_\alpha^0,q_\alpha'(0)\right),\quad \mathbf{Y}_0^h=\mathrm{col}\left(b_\beta^0,g_\beta'(0)\right),\\
\mathbf{F}_{irr}^e(t)&=\mathrm{col}\left(-j_\alpha^e,0\right),\quad \mathbf{F}_{irr}^h(t)=\mathrm{col}\left(-j_\beta^h,\omega_m^2\int_0^t j_\beta^h(t')dt'\right),
\end{aligned} \tag{20}$$

$$\mathbf{Q}_{sol}=\begin{pmatrix}0&\omega_n&1&0&0\\-\omega_n&0&0&0&1\\-\chi_e\omega_e^2&0&\gamma_e&0&0\\0&0&0&0&-1\\0&-\chi_m\omega_m^2&0&\omega_m^2&\gamma_m\end{pmatrix}$$

$$\mathbf{Q}_{irr}^e=\begin{pmatrix}0&1\\-\chi_e\omega_e^2&\gamma_e\end{pmatrix},\ \mathbf{Q}_{irr}^h=\begin{pmatrix}0&1\\-\mu_m\omega_m^2&\gamma_m\end{pmatrix},\ \mu_m=1+\chi_m.$$

This system of ODEs with constant coefficients (17)–(19) can be solved in a closed form [15]. Solenoidal mode amplitudes are obtained as

$$\mathbf{X}(t) = \sum_{k=1}^{5} \mathbf{K}\left(\lambda_k^{sol}\right) \left\{ e^{-t\cdot\lambda_k^{sol}} \mathbf{X}_0 + \int_0^t e^{-(t-t')\cdot\lambda_k^{sol}} \mathbf{F}_{sol}\left(t'\right) dt' \right\},$$

$$\mathbf{K}\left(\lambda_k^{sol}\right) = \prod_{s\neq k}^{s=1\ldots5} \frac{\lambda_s^{sol}\mathbf{I} - \mathbf{Q}_{sol}}{\lambda_s^{sol} - \lambda_k^{sol}}. \tag{21}$$

where λ_k^{sol} are eigenvalues of matrix $\mathbf{Q}_{sol}$ that can be found as roots of the characteristic equation

$$\begin{aligned} &\lambda^5 - (\gamma_m + \gamma_e)\,\lambda^4 + \left(\gamma_m\gamma_e + \chi_e\omega_e^2 + \mu_m\omega_m^2 + k_n^2\right)\lambda^3 \\ &- k_n^2\,(\gamma_m + \gamma_e)\,\lambda^2 - \left(\chi_e\omega_e^2\gamma_m + \mu_m\omega_m^2\gamma_e\right)\lambda^2 \\ &+ \left(\chi_e\mu_m\omega_e^2\omega_m^2 + k_n^2\left(\omega_m^2 + \gamma_m\gamma_e\right)\right)\lambda - k_n^2\omega_m^2\gamma_e = 0. \end{aligned} \tag{22}$$

The irrotational mode amplitudes are found asb

$$\mathbf{Y}^e(t) = \sum_{k=1}^{2} \mathbf{K}\left(\lambda_k^{irr(e)}\right) \left\{ e^{-t\cdot\lambda_k^{irr(e)}} \mathbf{Y}_0^e + \int_0^t e^{-(t-t')\cdot\lambda_k^{irr(e)}} \mathbf{F}_{irr}^e(t')dt' \right\}, \tag{23}$$

where

$$\begin{aligned} &\lambda_{1,2}^{irr(e)} = \frac{\gamma_e}{2} \mp i\omega_{irr}^e, \quad \omega_{irr}^e = \sqrt{\chi_e\omega_e^2 - \frac{\gamma_e^2}{4}}, \\ &\mathbf{K}\left(\lambda_1^{irr(e)}\right) = \frac{1}{2}\begin{pmatrix} -\frac{i\gamma_e}{2\omega_{irr}^e} + 1 & \frac{i}{\omega_{irr}^e} \\ -\frac{i\chi_e\omega_e^2}{\omega_{irr}^e} & \frac{i\gamma_e}{2\omega_{irr}^e} + 1 \end{pmatrix}, \\ &\mathbf{K}\left(\lambda_2^{irr(e)}\right) = \frac{1}{2}\begin{pmatrix} \frac{i\gamma_e}{2\omega_{irr}^e} + 1 & -\frac{i}{\omega_{irr}^e} \\ \frac{i\chi_e\omega_e^2}{\omega_{irr}^e} & -\frac{i\gamma_e}{2\omega_{irr}^e} + 1 \end{pmatrix}; \end{aligned}$$

and

$$\mathbf{Y}^h(t) = \sum_{k=1}^{2} \mathbf{K}\left(\lambda_k^{irr(h)}\right) \left\{ e^{-t\cdot\lambda_k^{irr(h)}} \mathbf{Y}_0^h + \int_0^t e^{-(t-t')\cdot\lambda_k^{irr(h)}} \mathbf{F}_{irr}^h(t')dt' \right\}, \tag{24}$$

where

$$\lambda_{1,2}^{irr(h)} = \frac{\gamma_m}{2} \mp i\omega_{irr}^h, \quad \omega_{irr}^h = \sqrt{\mu_m \omega_m^2 - \frac{\gamma_m^2}{4}}$$

$$\mathbf{K}\left(\lambda_1^{irr(h)}\right) = \frac{1}{2}\begin{pmatrix} -\frac{i\gamma_m}{2\omega_{irr}^h} + 1 & \frac{i}{\omega_{irr}^h} \\ -\frac{i\mu_m\omega_m^2}{\omega_{irr}^h} & \frac{i\gamma_m}{2\omega_{irr}^h} + 1 \end{pmatrix},$$

$$\mathbf{K}\left(\lambda_2^{irr(h)}\right) = \frac{1}{2}\begin{pmatrix} \frac{i\gamma_m}{2\omega_{irr}^h} + 1 & -\frac{i}{\omega_{irr}^h} \\ \frac{i\mu_m\omega_m^2}{\omega_{irr}^h} & -\frac{i\gamma_m}{2\omega_{irr}^h} + 1 \end{pmatrix}.$$

By substituting any specific initial conditions and time dependences for the impressed sources into this general form solution one can easily calculate the corresponding time dependences of the mode amplitudes and hence the sought electromagnetic fields.

Before calculating transient fields let us first study properties of the eigenfrequencies of the physical system under study.

3. EIGENFREQUENCIES OF SOLENOIDAL MODES

The first question of interest is the eigenvalues of the coefficient matrix $\mathbf{Q}_{sol}$ in the evolutionary equations — they are the eigenfrequencies of free oscillations in the cavity. The matrix 5×5 yields five eigenvalues — two complex conjugated pairs and one real eigenvalue. Imaginary parts of the eigenvalues (Fig. 2(a)) characterize frequencies of field oscillations; while the real parts (Fig. 2(b)) characterize damping of the corresponding oscillation component. The eigenfrequencies are plotted as functions of the cavity size expressed in terms of the empty cavity eigenfrequency (inverse proportional to its size).

There are two frequency ranges where free oscillations cannot exist — these are marked with gray strips in Fig. 2(a). Within these ranges $n'(f) < n''(f)$, the field have non-oscillating spatial distribution and can't satisfy zero boundary conditions at the cavity walls. The frequency marked as "1" in Fig. 2(a) can be defined as a 'cavity' frequency; it tends to the eigenfrequency of an empty cavity at high frequencies. The frequency marked as "2" can be defined as a 'medium' one, it corresponds roughly to the resonance frequency of the Lorentz permeability. This frequency lies in the negative refractive index frequency range. It corresponds to the area of anomalous dispersion, where the group velocity is positive, while the phase velocity is negative (Fig. 3). In contrast to the 'cavity' eigenfrequency the 'medium' eigenfrequency decreases with cavity size decrease. At this the cavity boundary doesn't affect the eigenfrequency significantly, especially it

is prominent at the low frequency limit around 6 GHz, where the group velocity tends to zero (Fig. 3). Oscillations at this frequency correspond to a wave that is bound to the place of excitation. That is the oscillating fields are formed as a "standing wave". This standing wave is formed not as interference of two opposite traveling waves rebouncing at the cavity walls but as a wave that travels at zero group velocity and thus doesn't care where the walls are placed.

It should be noted that in multimode regime all the higher modes have almost equal 'medium' eigenfrequencies (see Fig. 4). That is why quite arbitrary spatial distribution can be created at this frequency. The reason for this is near zero group velocity that prevents energy from spreading along the cavity, so almost any spatial energy distribution in initial conditions remains unchanged oscillating at the 'medium' frequency.

4. FREQUENCY RESPONSE OF THE CAVITY

Besides the eigenfrequencies the oscillating system can be characterized by its frequency response that describes amplitude of forced oscillations for a unit excitation at given frequency. The frequency response shows not only the position of the resonances but also their relative strength. In order to obtain it let us consider the governing equation

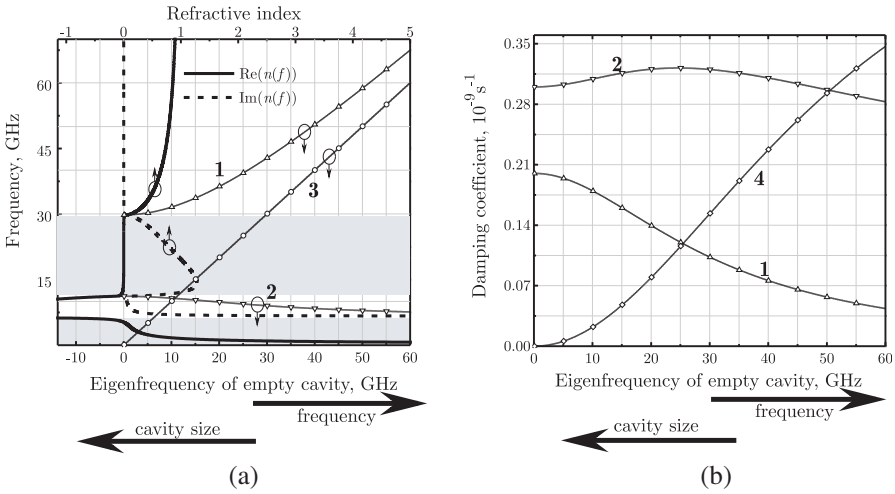

Figure 2. Imaginary and real part of eigenvalues of the filled cavity (1, 2, 4). Eigenfrequency of the empty cavity (3).

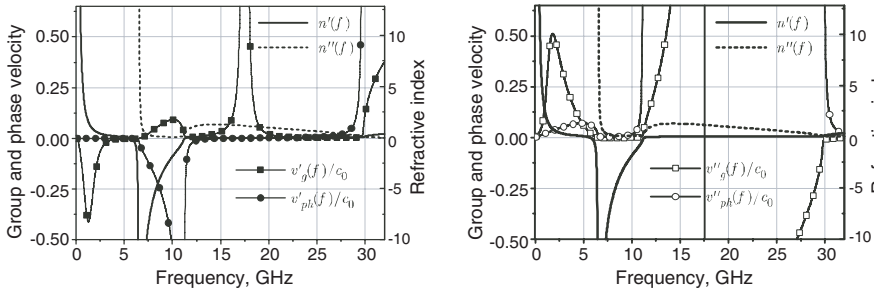

Figure 3. Dispersion characteristics of the medium. Real parts of the group and phase velocities is shown on left, while imaginary parts are shown on right. The group velocity loses its meaning in the regions with significant imaginary part.

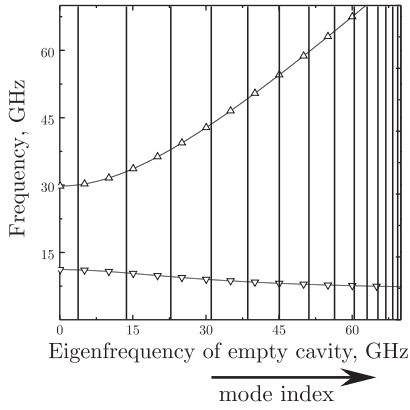

Figure 4. 'Cavity' and 'medium' frequency in multimode regime.

for solenoidal modes (17) written in the FD:

$$(i\omega\mathbf{I}+\mathbf{Q}_{sol})\cdot\tilde{\mathbf{X}}(\omega)=\tilde{\mathbf{F}}_{sol}(\omega),\quad \tilde{\mathbf{X}}(\omega)=\mathbf{R}(\omega)\,\tilde{\mathbf{F}}_{sol}(\omega),\quad \mathbf{R}(\omega)=(i\omega\mathbf{I}+\mathbf{Q}_{sol})^{-1} \tag{25}$$

where the frequency response matrix $\mathbf{R}(\omega)$ was introduced that relates complex amplitudes of the harmonic oscillations of the fields $\tilde{\mathbf{X}}(\omega)$ with those of the sources $\tilde{\mathbf{F}}(\omega)$. The first row of this matrix describes response to excitation by electric currents (see sources definition (20)). Some of these responses are shown in Fig. 5. One can clearly see two ridges on the plots that correspond to the 'cavity' and 'medium' eigenfrequencies discussed in the previous section. Peak amplitudes of these ridges for electric field response are shown separately in Fig. 5(c).

It can be seen that at large cavity size (low "Eigenfrequency of empty cavity") the 'medium' resonance is excited with much larger amplitude than the 'cavity' one, while with decrease of the cavity size the situation changes and the 'cavity' resonance becomes dominant for a small cavity.

An interesting feature can be observed at 30 GHz where neither electric field nor polarization can be excited for any cavity size (see valleys at Figs. 5(a) and 5(d)) while magnetic field and magnetization are though small but nonzero at this frequency. At this point the frequency derivatives of refractive index become infinite (see Figs. 2 and 3). A similar situation occurs for magnetic field at around 7 GHz: at Fig. 5(e) a valley exists at this frequency that doesn't depend on the cavity size. In contrast to situation with polarization that shares the valley with electric field, the magnetization response has no such valley at 7 GHz (Fig. 5(f)).

5. FORCED TRANSIENT OSCILLATIONS IN A CAVITY WITH DISPERSIVE DOUBLE NEGATIVE MEDIUM

Now let us consider transient processes that occur in the cavity under pulse excitation by electric currents with the following waveform

$$j_\alpha^e(t) = j_n^e(t) = \left(\frac{t}{T}\right)^2 \left(1 - \frac{t}{3T}\right) e^{-t/T} \times Heaviside(t). \tag{26}$$

This waveform is shown in Fig. 6. In numerical calculations we used two such signals with parameter T set so that signal spectrum was allocated around the 'medium' frequency for the first signal and around the 'cavity' frequency for the second one (see Fig. 7).

By substituting time dependence (26) into (21)–(24) a closed-form waveforms for the solenoidal mode amplitudes is obtained as:

$$\begin{aligned} \mathbf{X}(t) &= \sum_{k=1}^{5} I\left(\lambda_k^{sol}, t\right) \mathbf{K}\left(\lambda_k^{sol}\right) \cdot \mathrm{col}\,(1,0,0,0,0) \\ \mathbf{K}\left(\lambda_k^{sol}\right) &= \prod_{s\neq k}^{s=1\ldots5} \frac{\lambda_s^{sol}\mathbf{U} - \mathbf{Q}_{sol}}{\lambda_s^{sol} - \lambda_k^{sol}}. \end{aligned} \tag{27}$$

where λ_k^{sol} are the roots of (22), the function $I(\lambda, t)$ is defined as

$$\begin{aligned} I(\lambda,t) \;=\; & \frac{-Te^{-t/T}}{\lambda T - 1}\left\{\frac{1}{3}\left(\frac{t}{T}\right)^3 - \frac{\lambda T\left(\frac{t}{T}\right)^2}{\lambda T - 1} + \frac{2\lambda t}{(\lambda T-1)^2} - \frac{2\lambda T}{(\lambda T-1)^3}\right\} \\ & - \frac{2\lambda T^2 e^{-\lambda t}}{(\lambda T - 1)^4} \end{aligned}$$

Electric irrotational mode amplitudes are found as

$$a_\alpha(t) = \frac{1}{2}\left(1 - \frac{i\gamma_e}{2\omega^e_{irr}}\right) I\left(\lambda^e_{irr1}, t\right) + \frac{1}{2}\left(1 + \frac{i\gamma_e}{2\omega^e_{irr}}\right) I\left(\lambda^e_{irr2}, t\right) \quad (28)$$

$$q'(t) = \frac{i\chi_e\omega_e^2}{2\omega^e_{irr}}\left(I\left(\lambda^e_{irr2}, t\right) - I\left(\lambda^e_{irr1}, t\right)\right) \quad (29)$$

$$\lambda^e_{irr1,2} = \frac{\gamma_e}{2} \mp i\omega^e_{irr}, \quad \omega^e_{irr} = \sqrt{\chi_e\omega_e^2 - \frac{\gamma_e^2}{4}}$$

Since the sources (26) are chosen to be only of electric type ($j^h_n(t)$, $j^h_\beta(t)$ are assumed to be zero) the magnetic irrotational part of the field is not excited.

The cavity size is chosen such that its 'empty' eigenfrequency is 10.7 GHz, at this the resulting 'medium' eigenfrequency is the same (Fig. 7). 'Cavity' eigenfrequency is 31.8 GHz. Quality factors were found to be 1127 for the 'cavity' frequency and 216 for the 'medium' frequency. In spite of higher Q-factor one can see from Fig. 5(c) that

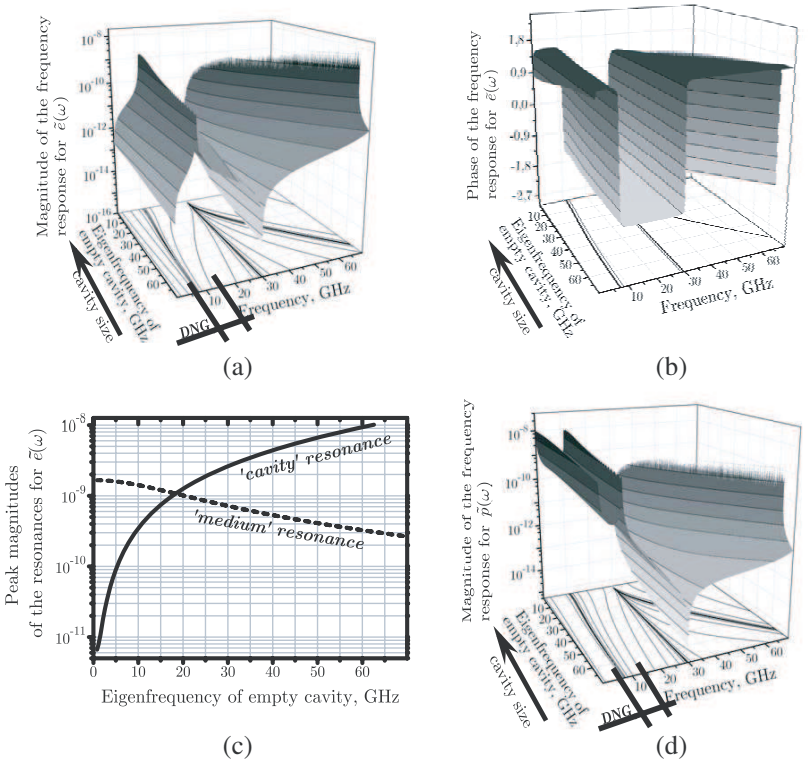

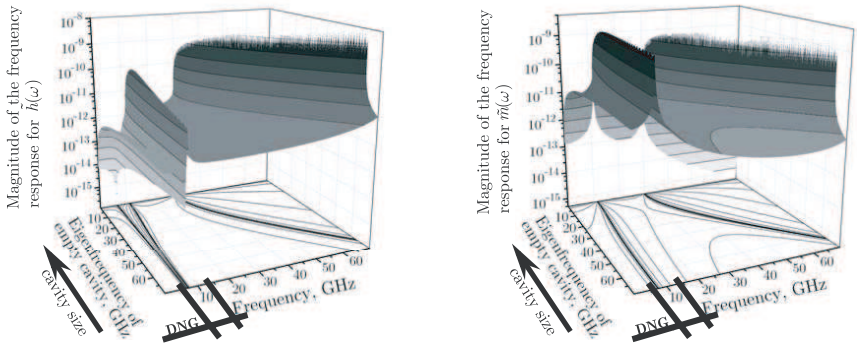

(e) (f)

Figure 5. Frequency responses of the cavity as function of cavity size (given by "Eigenfrequency of empty cavity") for excitation by electric current. (a) Magnitude of the response for electric field mode de amplitude $\tilde{e}(\omega)$. (b) Phase of the frequency response for electric field mode amplitude $\tilde{e}(\omega)$. (c) Peak magnitudes of the resonances at the response for $\tilde{e}(\omega)$ (peak values of the ridges at plot a). (d) Magnitude of the frequency response for electric polarization mode amplitude $\tilde{p}(\omega)$. (e) Magnitude of the frequency response for magnetic field mode amplitude $\tilde{h}(\omega)$. (f) Magnitude of the frequency response for magnetization mode amplitude $\tilde{m}(\omega)$.

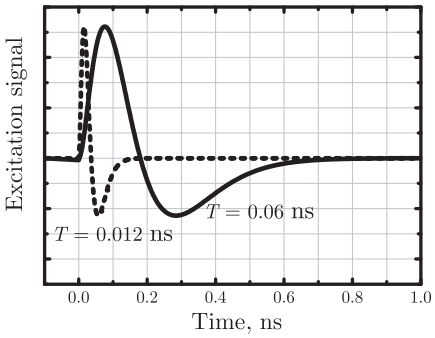

Figure 6. Time dependence of the excitation signals.

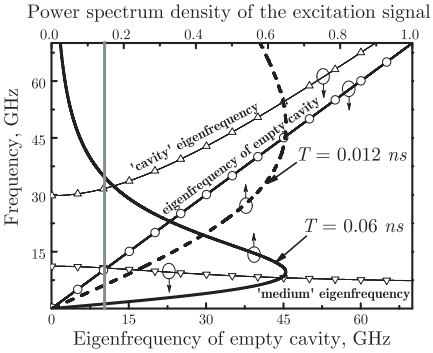

Figure 7. Power spectrum density of the excitation signals.

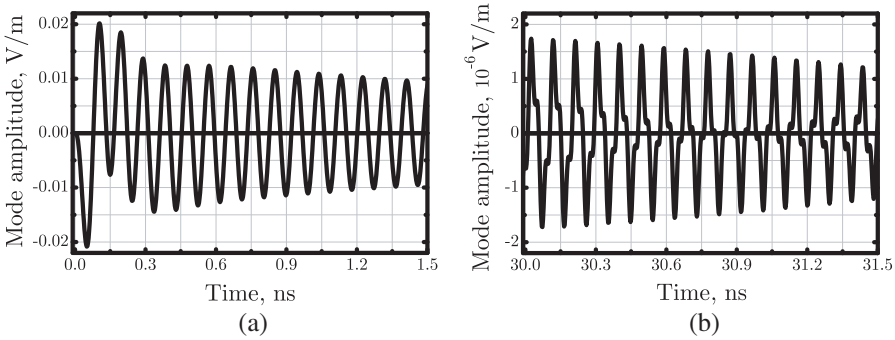

Figure 8. Time oscillations of the mode amplitude $e_n(t)$, for a long pulse with $T = 0.06$ ns.

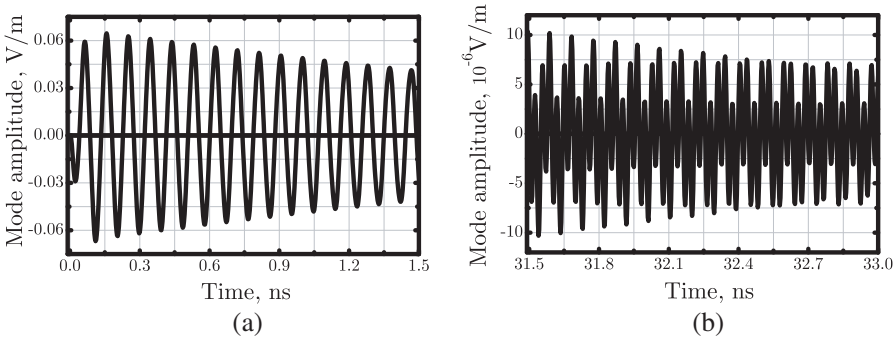

Figure 9. Time oscillations of the mode amplitude $e_n(t)$, for a short pulse with $T = 0.012$ ns.

the 'cavity' resonance has much smaller response than the 'medium' one. Though the two excitation signals are chosen to have maximum spectral density at two distinct resonances but in the time evolution we can observe that at early time only 'medium' frequency is excited due to much higher response (Figs. 8 and 9). Only at late time the 'cavity' eigenfrequency becomes visible at background because it decays at smaller rate due to higher Q-factor.

6. CONCLUSION

A cavity with double negative medium has been considered both in Frequency and Time Domains. The solution has been carried out based on mode decomposition of the fields. A closed-form solution in TD has been obtained for transient oscillations in the cavity. Frequency responses for mode amplitudes have been analyzed and the following

features have been revealed:

- there are two complex eigenfrequencies for a mode that correspond to 'cavity' and 'medium' resonances;
- 'medium' eigenfrequency has very little dependence on the cavity size, it corresponds to the frequency band where medium has double negative properties;
- there are frequency bands where resonances do not occur for any cavity size;
- there are specific frequencies where either electric or magnetic field response is close to zero for any cavity size, these two frequency points correspond to very high frequency derivatives of refractivity;
- at large cavity size the peak amplitude of the 'cavity' resonance tends to zero, while at small cavity size it significantly dominates over the 'medium' resonance.
- the 'medium' resonance frequency slightly decreases with decrease in cavity size in contrast to close to linear increase in the 'cavity' eigenfrequency;
- The 'medium' oscillation occurs at almost the same frequency for all modes and any cavity size. It can be explained by locality of energy due to close to zero group velocity, so the oscillations occur locally and depend only on the medium properties but not on the cavity boundaries.

In spite of high losses supposed to be observed in the region of anomalous dispersion a relatively high quality factor $Q_m \approx 200$ was obtained at DNG frequency band within a rather realistic dispersion model used in calculations.

The main intent of this paper was to show that dispersion **should** be taken into account when analyzing resonance structures with DNG medium because behavior of such systems is determined by complex interaction of medium and structure resonances that can bring in some new unexpected effects.

REFERENCES

1. Veselago, V. G., "The electrodynamic of substance with simultaneously negative values of ε and μ," *Usp. Sov. Phys.,* Vol. 10, No. 4, 509–514, 1968.
2. Engheta, N. and R. W. Ziolkowski, "A positive future for double-negative metamaterials," *IEEE Trans. Microwave Theory Tech.*, Vol. 53, No. 4, 1535–1556, 2005.
3. Bozza, G., G. Oliveri, and M. Raffetto, "Anomalous TEM modes in guiding structures filled with double negative and

double positive materials," *IEEE Microwave Wireless Comp. Lett.*, Vol. 17, No. 1, 19–21, 2007.

4. Marcos, P. and C. M. Soukoulis, "Transmission properties and effective electromagnetic parameters of double negative metamaterials," *Optic Express*, Vol. 11, No. 7, 649–661, 2003.
5. Vendik, I., O. Vendik, I. Kolmakov, and M. Odit, "Modelling of isotropic double negative media for microwave applications," *Opto-Electronics Review*, Vol. 14, No. 3, 179–186, 2006.
6. Grzegorczyk, T. M. and J. A. Kong, "Review of left-handed metamaterials: Evolution from theoretical and numerical studies to potential applications," *Journal of Electromagnetic Waves and Applications*, Vol. 20, No. 14, 2053–2064, 2006.
7. Chen, H., B. I. Wu, and J. A. Kong, "Review of electromagnetic theory in left-handed materials," *Journal of Electromagnetic Waves and Applications*, Vol. 20, No. 15, 2137–2151, 2006.
8. Engeta, N., "An idea for thin subwavelength cavity resonators using metamaterials with negative permittivity and permeability," *IEEE Trans. Antennas Propag.*, Vol. 50, No. 1, 10–12, 2002.
9. Li, Y., L. Ran, H. Chen, J. Huangfu, X. Zhang, K. Chen, T. M. Grzegorczyk, and J. A. Kong, "Experimental realization of a one-dimensional LHM-RHM resonator", *IEEE Trans. Microwave Theory Tech.*, Vol. 53, No. 4, 1522–1526, 2005.
10. Hand, T., S. Cummer, and N. Engeta, "The measured electric field spatial distribution within a metamaterial subwavelength cavity resonator," *IEEE Trans. Antennas Propag.*, Vol. 55, No. 6, 1781–1788, 2007.
11. Bozza, G., G. Oliveri, and M. Raffetto, "Cavities involving metamaterials with an uncountable set of resonant frequencies," *IEEE Microwave and Wireless Comp. Lett.*, Vol. 17, No. 8, 565–567, 2007.
12. Tretyakov, O. A., "The method of modal basis," *Radiotechnika i Elektronika*, Vol. 31, 1071–1082, 1986.
13. Tretyakov, O. A., "Essentials of nonstationary and nonlinear electromagnetic field theory," *Analytical and Numerical Methods in the Electromagnetic Wave Theory*, M. Hashimoto, M. Idemen, O. A. Tretyakov (eds.), Science House Co., Ltd., Tokyo, 1993.
14. Tretyakov, O. A. and F. Erden, "Temporal cavity oscillations caused by a wide-band waveform," *Progress In Electromagnetics Research B*, Vol. 6, 183–204, 2008.
15. Ango, A., *Mathematics for Electric and Radio Engineers*, Nauka, Moscow, Russian, 1965.